Preprints, 10th IFAC International Symposium on
Advanced Control of Chemical Processes
Shenyang, Liaoning, China, July 25-27, 2018

Power Maximization of Wind Farms using Discrete-time Distributed Extremum Seeking Control

Judith Ebegbulem * **Martin Guay** *

* *Department of Chemical Engineering, Queen's University Kingston, ON, K7L 3N6, Canada (e-mail: guaym@queensu.ca).*

Abstract: The use of a model independent control approach to tackle the problem of wind farm power maximization under constant and varying free stream wind speed and direction is considered. In this paper, a time-varying extremum seeking control (TVESC) for discrete-time systems is utilized in a distributed and a collaborative manner. Each controller monitors the actions of a wind turbine and the objective is to maximize the farm wide power capture. To address this task, the distributed controllers ensure that the turbines share local information over an undirected connected communication network. Also, with the use of a discretized version of a continuous-time dynamic average consensus estimator, the controllers help the turbines estimate the mean of the overall power generated in the wind farm. The dynamics of each turbine power estimate is parameterized and the unknown gradient is estimated as a time-varying parameter using a tailored estimation routine. This information is used in the design of the extremum seeking controller. The problem to be solved is addressed via numerical simulations, results are provided to show the effectiveness of this technique.

Keywords: Wind farm, model independent, discrete-time, distributed extremum seeking control, dynamic average consensus estimator.

1. INTRODUCTION

The environmental effects associated with the use of fossil fuels for power generation can be effectively avoided if more attention is given to the issue of generating power from wind energy. Wind energy is clean and renewable. In a wind farm, the turbines trap energy from the wind for power generation. One of the challenges limiting maximum power capture is the aerodynamic wake interactions between the wind turbines. Efforts have been made to overcome this challenge. Optimizing the layout of wind farms has been considered as an effective way of reducing these interactions (see Chowdhury et al. (2012), Chowdhury et al. (2013), Pérez et al. (2013), Dupont and Cagan (2012), Dupont et al. (2016) and Liu and Wang (2014)).

As noted in Chowdhury et al. (2012) and Chowdhury et al. (2013), the unrestricted wind farm layout optimization method allows for optimal selection and positioning of wind turbines such that the wind farm power is maximized. The combination of an heuristic method with nonlinear mathematical programming techniques for optimal offshore wind farm layout was put forward in Pérez et al. (2013). An Extended Pattern Search (EPS) technique (which integrates deterministic algorithms with stochastic methods) was proposed in Dupont and Cagan (2012). In Dupont and Cagan (2012), it was mentioned that more power was generated from a layout designed with the EPS technique than earlier investigated techniques using the same aerodynamic wake interaction models and cost functions. The work carried out in Dupont et al. (2016) proposes the use of an Extended pattern Search-Multi-Agent System (EPS-MAS) with an advanced wind farm modelling system. In addition to wind farm layout optimization, wake models have been developed to account for the aerodynamic interactions (Jensen (1983), Torres et al. (2011) and Troldborg et al. (2010) and Dupont et al. (2016)). The offshore wind farm model employed in Dupont et al. (2016) takes into account the cost of installation of the wind farm and the effect of shear on wind speed and wake propagation. Also, it considered the effects of atmospheric stability and the possibility of partial wake interactions among the turbines.

At this point, it is important to mention that there are no models that accurately describe the aerodynamic interactions. One way to overcome this challenge would be to utilize a model independent control technique for maximum wind farm power capture. Two model independent control techniques (Marden et al. (2013) and Menon and Baras (2014)) have been utilized to address such a problem. In Marden et al. (2013), two game theoretic distributed learning algorithms were put forward (safe experimentation dynamics and payoff-based distributed learning for Pareto optimality). The perturbation based extremum seeking control technique (PBESC) was employed in Menon and Baras (2014). The power maximization problems tackled in these research papers were addressed in a distributed fashion and under constant free stream wind speed and direction conditions.

In this paper, we employ a different extremum seeking control technique (a TVESC technique put forward in Guay (2014) for discrete-time systems) for wind farm

Copyright © 2018 IFAC

power maximization. Extremum seeking Control (ESC) is a gradient based and an adaptive control technique. It is a real-time optimization technique that tracks the optimum of an unknown but measured cost or objective function. Extremum seeking control has been applied to address problems associated with resource allocation Poveda and Quijano (2013), source seeking Ghods et al. (2010), brake systems Zhang and Ordóñez (2012), chilled water plants Sane et al. (2006) and formation control Vandermeulen et al. (2017).

The TVESC technique to be employed involves estimating the gradient of an unknown cost function as a time-varying parameter followed by the design of a controller that solves the optimization task. Our main contribution is the implementation of this technique in a distributed and a cooperative manner and its utilization in solving the power maximization problem of a wind farm. In addition, this problem is addressed under fixed and varying free stream wind speed and direction. Distributed control is chosen as it allows for the use of multiple TVESC controllers such that each controller monitors the actions of a single turbine in the wind farm. Through communication, the controllers work to optimize the overall power generated by the wind farm.

The paper is organized as follows. The problem description is given in Section 2. The wind farm model is presented in Section 3. The distributed TVESC technique is described in Section 4. Simulation results are provided in Section 5 and concluding remarks made in Section 6.

2. PROBLEM DESCRIPTION

The optimization problem to be solved is given by:

$$\max_{u[k]\in\mathbb{R}^p} Y(u[k]) \tag{1}$$

s.t.

$$Y(u[k]) = \sum_{i=1}^{p} y_i(u[k]). \tag{2}$$

A wind farm with p number of wind turbines is considered. Let $i = 1, \dots, p$ and k be the time step. Also, let $u[k]$ be the vector of axial induction factors for the turbines (the vector of input variables) at the kth time step taking values in a convex and compact set $\mathcal{U} \subset \mathbb{R}^p$. The unknown function $Y(u[k])$ represents the power generated in the wind farm (and can be referred to as the overall cost) at the kth time step and depends on $u[k]$. $Y(u[k])$ is assumed to smooth. $J[k] = Y(u[k])$ is the measured value of $Y(u[k])$. $y_i(u[k])$ is the unknown function representing the power generated (local cost) by turbine i at the kth time step and $q_i[k]$ is the measured value of $y_i(u[k])$. To tackle the stated maximization problem, we make the following assumptions.

Assumption 1. Agent i has access to its axial induction factor u_i and the measured value q_i.

Assumption 2. Let u^* be the unique maximizer of problem (1) then $Y(u)$ is strongly concave, i.e.,

$$(u - u^*)^\top \frac{\partial Y(u)}{\partial u} \le -\gamma_1 \|u - u^*\|^2 \tag{3}$$

$\forall u \in \mathcal{U}$ with $\gamma_1 > 0$.

Remark 1. Recall that $Y(u)$ is smooth by assumption, it follows that it satisfies:

$$\|Y(u)\| \le \gamma_2, \quad \left\|\frac{\partial Y(u)}{\partial u}\right\| \le L_1, \quad \left\|\frac{\partial^2 Y(u)}{\partial u \partial u^\top}\right\| \le L_2, \tag{4}$$

$\forall u \in \mathcal{U}$ with γ_2, L_1, $L_2 > 0$.

3. WIND FARM MODEL

The model of the wind farm used for simulation is presented in this Section. Note that it is described for the sole purpose of simulation, the distributed TVESC has no knowledge of the model. Consider the wind farm given in

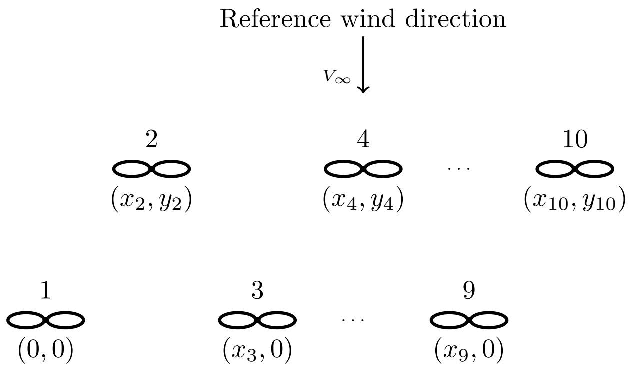

Fig. 1. The orientation of the wind farm with ten turbines.

Figure 1. The turbines are originally located at coordinates $\{(x_1, y_1), \dots, (x_{10}, y_{10})\}$ from a common point and a reference wind direction. It is assumed that the turbines are identical which means that they are of the same diameter. Let $V_G = \{1, \dots, 10\}$ denote the set of turbines in the wind farm. It is referred to as the vertex set. Let V_{G_u} and V_{G_d} be the sets of upstream and downstream turbines respectively then $V_{G_u} = \{m \in V_G : m \text{ is upstream}\}$ and $V_{G_d} = \{n \in V_G : n \text{ is downstream}\}$. To proceed, the following assumptions are required.

Assumption 3. The wind farm is oriented and the reference wind direction is the negative vertical direction.

Assumption 4. When the wind is in the reference direction or when it changes β degrees clockwise away from the reference direction, only turbine $n \in V_{G_d}$ such that $n = m - 1$ for $m \in V_{G_u}$ can be partially or totally in the wake of turbine m.

3.1 Power Model

According to Manwell et al. (2002), the power generated by a turbine is of the form:

$$y_i(u) = \frac{1}{2}\rho_{air} a_i C_{p_i} V_i^3 \tag{5}$$

where:

- $\rho_{air} = 1.225\ kg/m^3$ is the density of air;
- a_i = area of disk generated by the blades of turbine i in m^2;
- C_{p_i} = power efficiency coefficient for turbine i;
- V_i = wind speed at turbine i in (m/s).

3.2 Power Efficiency Coefficient

The power efficiency coefficient for turbine i is given by:

$$C_{p_i} = 4u_i(1-u_i)^2. \tag{6}$$

- u_i = axial induction factor for turbine i. As recorded in Marden et al. (2013), it gives a measure of the decrease in wind velocity through the turbine.

3.3 Wake Interaction Model

As presented in Grunnet et al. (2010), the wind speed at turbine i takes the form:

$$V_i \approx \delta V_\infty \tag{7}$$

where:

- V_∞ = free stream wind speed in (m/s);
- δ = wind speed deficit seen at turbine i.

Note that if $i = m$, $V_i \approx V_\infty$. If $i = n$ then the wind speed deficit δ is given by:

$$\delta \approx 1 - \frac{O_{m,n} C_{T_m}}{2a_n(1+\frac{\tilde{y}_{m,n}}{4r_n})}. \tag{8}$$

Also, note that:

- r_n is the radius (m) of the disk generated by the blades of turbine n.
- $\tilde{y}_{m,n} = \tilde{y}_m - \tilde{y}_n$ represents the vertical distance between upstream turbine m and downstream turbine n after the wind direction changes β clockwise from the reference wind direction.
- According to Pérez et al. (2013), the new coordinates $\tilde{x}_i$ and $\tilde{y}_i$ for turbine i are obtained as follows:

$$\begin{bmatrix} \tilde{x}_i \\ \tilde{y}_i \end{bmatrix} = \begin{bmatrix} \cos\beta & -\sin\beta \\ \sin\beta & \cos\beta \end{bmatrix} \begin{bmatrix} x_i \\ y_i \end{bmatrix}. \tag{9}$$

- $O_{m,n}$ is the area of overlap between the wake of turbine m and the disk produced by the blades of turbine n. The wake expansion of turbine m (e_{w_m}) as noted in Grunnet et al. (2010) is of the form (10).

$$\begin{aligned} e_{w_m} &= 2r_m\sqrt{1+\frac{\tilde{y}_{m,n}}{4r_m}} \\ r_{w_m} &= \frac{e_{w_m}}{2} \end{aligned} \tag{10}$$

with r_{w_m} being the radius of e_{w_m}. According to Liu and Wang (2014), $O_{m,n}$ is of the form:

$$O_{m,n} = \left\{ \begin{array}{ll} 0, & \tilde{x}_{m,n} > r_{w_m} + r_n \\ \pi r_n^2, & \tilde{x}_{m,n} < r_{w_m} - r_n \\ \tau_1, & r_{w_m} < \tilde{x}_{m,n} < r_{w_m} + r_n \\ \tau_2, & r_{w_m} - r_n < \tilde{x}_{m,n} < r_{w_m} \end{array} \right\}$$

where $\tau_1 = F_1 + F_2 - F_3$ and $\tau_2 = \pi\mu_3^2 - (F_1 - F_4 - F_3)$ and $\tilde{x}_{m,n} = \tilde{x}_m - \tilde{x}_n$. $\tilde{x}_{m,n}$ is the horizontal distance between turbines m and n after a change in wind direction. Let $\mu_1 = r_{w_m}$, $\mu_2 = r_n$ and $\mu_3 = \tilde{x}_{m,n}$, $\beta_1 = arc\cos\frac{\mu_1^2+\mu_3^2-\mu_2^2}{2\mu_1\mu_3}$, $\beta_2 = arc\cos\frac{\mu_3^2+\mu_2^2-\mu_1^2}{2\mu_2\mu_3}$ and $\beta_3 = 180^\circ - arc\cos\frac{\mu_3^2+\mu_2^2-\mu_1^2}{2\mu_2\mu_3}$. $F_1 = \frac{\beta_1}{180^\circ}\pi\mu_1^2$, $F_2 = \frac{\beta_2}{180^\circ}\pi\mu_2^2$, $F_3 = \mu_1\mu_3\sin\beta_1$ and $F_4 = \frac{\beta_3}{180^\circ}\pi\mu_2^2$;

- C_{T_m} is the thrust coefficient for turbine m. It takes the form:

$$C_{T_m} = 4u_m(1-u_m); \tag{11}$$

4. DISTRIBUTED EXTREMUM SEEKING CONTROL

4.1 Communication Network

The communication network for the wind farm is given in Figure 2. It is designed as a time-invariant undirected connected graph $G = (V_G, E_G)$. $E_G \subset V_G \times V_G$ represents the edge set, an edge connects two turbines and acts as the pathway for communication. We allow local commuincation between turbines (they share their power information with their neighbours) to demonstrate that global communication is not required to address the optimation task. Turbines i and j can communicate means $(i,j) \in E_G \Leftrightarrow (j,i) \in E_G$ and $(i,j) \notin E_G \Leftrightarrow (j,i) \notin E_G$ means otherwise. Also, if turbines i and j can communicate, it means they are neighbours. Let N_i denote the set of turbine i's neighbours, then mathematically, we can say $\forall i,\, j \in V_G\colon N_i = \{j\colon (i,j) \in E_G\}$.

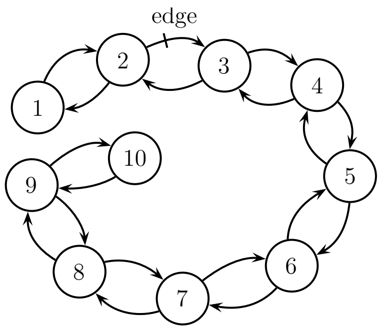

Fig. 2. Undirected communication network G for the ten turbine wind farm

4.2 Consensus Estimation

To address the optimization task (1), the turbines are required to estimate the average of the overall power generated in the wind farm. Let agent i's estimate of this average be $\hat{h}_i$ and the true average be h_i given by:

$$h_i[k] = \frac{1}{p}J[k] \tag{12}$$

To obtain $\hat{h}_i[k]$, a discrete-time dynamic average consensus estimator (DDACE) is needed. we employ a discretized version of the continuous-time proportional-integral dynamic average consensus estimator proposed in Freeman et al. (2006). The DDACE takes the form:

$$\begin{bmatrix} \hat{h}[k+1] \\ c[k+1] \end{bmatrix} = \left(I + \delta \begin{bmatrix} -I\gamma - k_P L & -k_I L^\top \\ -k_I L & 0 \end{bmatrix} \right) \begin{bmatrix} \hat{h}[k] \\ c[k] \end{bmatrix} + \delta \begin{bmatrix} I\gamma \\ 0 \end{bmatrix} q[k] \tag{13}$$

where $\hat{h} = [\hat{h}_1, ..., \hat{h}_p]^\top$, $c = [c_1, ..., c_p]^\top$ is a vector of auxiliary variables, I is $p \times p$ identity matrix, k_P, k_I, γ and δ_1 are positive constants to be assigned. Note that δ is required to be very small while γ, k_P and k_I are chosen to be large (much larger than the ESC gains). This is because the consensus routine must operate at a faster time-scale than the ESC algorithm. The Laplacian matrix $L \in \mathbb{R}^{p\times p}$ is defined as $L = D - A$. $D \in \mathbb{R}^{p\times p}$ is a degree matrix with diagonal elements equal to the number of neighbours of each corresponding turbine i. $A \in \mathbb{R}^{p\times p}$ is an adjacency matrix with element $a_{i,j} = 1$ if turbines i and j can communicate and 0 otherwise. Note that $a_{i,j} = 0$ if $j = i$.

4.3 Parametrization of the dynamics of h_i

Note that $\Delta h_i[k] = h_i[k+1] - h_i[k]$ and can be parameterized as:

$$\Delta h_i[k] = \sum_{j\neq i} \Delta u_j[k] \int_0^1 \frac{\partial h_i}{\partial u_j}\big(\lambda u_j[k+1] + (1-\lambda)u_j[k]\big)d\lambda + \Delta u_i[k] \int_0^1 \frac{\partial h_i}{\partial u_i}\big(\lambda u_i[k+1] + (1-\lambda)u_i[k]\big)d\lambda \tag{14}$$

where $\Delta u_i[k] = u_i[k+1] - u_i[k]$ and $\Delta u_j[k] = u_j[k+1] - u_j[k]$. Let $\theta_{0,i}[k] = \sum_{j\neq i} \Delta u_j[k] \int_0^1 \frac{\partial h_i}{\partial u_j}\big(\lambda u_j[k+1] + (1-\lambda)u_j[k]\big)d\lambda$ and $\theta_{1,i}[k] = \int_0^1 \frac{\partial h_i}{\partial u_i}\big(\lambda u_i[k+1]+(1-\lambda)u_i[k]\big)d\lambda$, (14) can be rewritten as:

$$\Delta h_i[k] = \theta_{0,i}[k] + \theta_{1,i}[k]\Delta u_i[k] = \phi_i^\top[k]\theta_i[k]. \tag{15}$$

Note that $\theta_{0,i}[k]$ represents the effect of drift and the other turbines on $h_i[k]$ while $\theta_{1,i}[k]$ measures the gradient of $h_i[k]$ with respect to its input $u_i[k]$. $\theta_i[k] = \big[\theta_{0,i}[k], \theta_{1,i}[k]\big]^\top$ is the vector of time-varying parameters and the regressor vector $\phi_i[k] = \big[1, \Delta u_i[k]\big]^\top$.

4.4 Parameter Estimation Routine

Observe that what we have is $\Delta\hat{h}_i[k]$ and not Δh_i[k]. Consequently, $\theta_i[k]$ is unknown. The parameter estimation approach given in Guay (2014) will be utilized to accurately estimate $\theta_i[k]$.

Let $\hat{\theta}_i[k] = \big[\hat{\theta}_{0,i}[k], \hat{\theta}_{1,i}[k]\big]^\top$ be the vector of parameter estimates. We denote the predicted output for a given value of the estimate $\hat{\theta}_i[k]$ as $\Delta\hat{z}_i[k]$ and the output prediction error as $e_i[k]$ with $e_i[k] = \Delta\hat{h}_i[k] - \Delta\hat{z}_i[k]$. The estimator model for (15) is written as:

$$\Delta\hat{z}_i[k] = \phi_i^\top[k]\hat{\theta}_i[k], \quad \Delta\hat{z}_i[0] = \Delta\hat{h}_i[0]. \tag{16}$$

The covariance matrix $\Sigma_i[k+1] \in \mathbb{R}^{2\times 2}$ is generated from:

$$\Sigma_i[k+1] = \alpha\Sigma_i[k] + \phi_i[k]\phi_i[k]^\top, \quad \Sigma_i[0] = \alpha I > 0 \tag{17}$$

where α is a small positive number chosen between 0 and 1 to ensure that Σ_i remains bounded. The parameter update law is given by:

$$\Sigma_i^{-1}[k+1] = \frac{1}{\alpha}\Sigma_i^{-1}[k] - \frac{1}{\alpha^2}\Sigma_i^{-1}[k]\phi_i[k]\big(1+ \frac{1}{\alpha}\phi_i^\top[k]\Sigma_i^{-1}[k]\phi_i[k]\big)^{-1}\phi_i^\top[k]\Sigma_i^{-1}[k] \tag{18}$$

where $\Sigma_i^{-1}[0] = \frac{1}{\alpha}I$.

$$\hat{\theta}_i[k+1] = \text{Proj}\,\big(\hat{\theta}_i[k] + \frac{1}{\alpha}\Sigma_i^{-1}[k]\phi_i[k]\,(1+ \frac{1}{\alpha}\phi_i^\top[k]\Sigma_i^{-1}[k]\phi_i[k])^{-1}e_i[k], \Theta\big) \tag{19}$$

where $\hat{\theta}_i[0] \in \Theta$ and Θ is a ball of finite radius centred at the origin. The projection operator denotes an orthogonal projection onto the surface of the uncertainty set. According to Goodwin and Sin (2013), the application of the operator is such that:

$$\hat{\theta}_i[k+1] \in \Theta, \quad \forall k \geq 0.$$

The signals of the closed-loop ESC system must be such that the following Persistence of Excitation condition is met.

Assumption 5. According to Goodwin and Sin (2013), there exist constants α_1 and $T > 0$ such that

$$\frac{1}{T}\sum_{g=k}^{k+T-1} \phi_i[g]\phi_i^\top[g] > \alpha_1 I, \quad \forall k > T. \tag{20}$$

4.5 Distributed Extremum Seeking Controller Design

The distributed TVESC is designed as follows:

$$u_i[k+1] = u_i[k] + k_g\hat{\theta}_{1,i}[k] + d_i[k] \tag{21}$$

where $k_g > 0$ is the optimization gain and $d_i[k]$ is the bounded dither signal (with amplitude σ and frequency ω_i) for turbine i. A small value for k_g is required to provide the required response. Making k_g large can increase the convergence speed but can also cause some unwanted system behaviour. To meet the Persistence of Excitation condition, sinusoidal dither signals with different frequencies are utilized. d_i is such that $\|d_i[k]\| \leq \zeta_i\ \forall k \geq 0$. Note that $\zeta_i > 0$.

5. APPLICATION TO WIND FARM POWER MAXIMIZATION

5.1 Example 1

Consider the wind farm described in Section 3. The turbines have the same radius ($r_i = r = 70\,m$) and are located at coordinates $\{(0,0), (10r, 30r), (20r, 0), \cdots, (90r, 30r)\}$. Wind is blowing in the reference wind direction at a constant free stream wind speed of 10 m/s ($V_\infty = 10\,m/s$). The goal is to maximize the total power generated by the turbines. The Laplacian matrix L for the wind farm is given by:

$$L = \begin{bmatrix} 1 & -1 & 0 & \dots & 0 \\ -1 & 2 & -1 & \dots & 0 \\ 0 & -1 & 2 & \dots & 0 \\ \vdots & \vdots & \vdots & \ddots & \vdots \\ 0 & 0 & 0 & \dots & 1 \end{bmatrix}$$

The tuning parameters were chosen as: $\delta_1 = 1 \times 10^{-3}$, $\alpha = 3 \times 10^{-3}$, $k_g = 2 \times 10^{-3}$, $\sigma = 1 \times 10^{-5}$ and $\omega = [67, 61, 55, \cdots, 21, 18]^\top$, $\gamma = 30$, $k_P = k_I = 250$. The control algorithm was initiated at: $u_i[0] = 0.1$, $\hat{\theta}_i[0] = [0.001, 0]^T$, $\Sigma_i[0] = \alpha I_{2\times 2}$, , $c_i[0] = 0$ and $\Delta\hat{h}_i[0] = \Delta\hat{z}_i[0] = 0$. The simulation result is seen in Figure 3.

For example 1, observe that positioning the turbines at those coordinates prevents wake interactions and allows the turbines to use the free stream wind speed. In this case, $O_{m,n} = 0$. $J^* = 5.5874 \times 10^7$ Watts and $u^* = [0.3333, \cdots, 0.3333, 0.3333]^\top$, that is $u_i^* = 0.3333$. This is optimal for a wind farm without wake interference and as such maximizes the overall power produced. The result obtained is presented in Figure 3, the distributed extremum seeking controllers ensure that this optimum is located.

5.2 Example 2

Case 1: The wind direction changes 13°clockwise from the reference direction after 200 seconds.

Case 2: The wind direction changes 15°clockwise from the reference direction after 300 seconds.

Using L, the initial conditions and the tuning parameters given above, we demonstrate that the TVESC technique can be used to maximize the farm wide power capture. The simulation results for case 1 and case 2 are presented in Figures 4 and 5 respectively.

For case 1, $J^* = 5.4021 \times 10^7$ Watts and $u^* = [0.3333, \cdots, 0.3258]^\top$. That is $\forall i \in V_{G_d} : u_i^* = 0.3333$ while $\forall i \in V_{G_u} : u_i^* = 0.3258$. Observe from Figure 4 that for the first 200 seconds, the turbines use the free stream wind speed (as there are no wake interactions) so the power generated in the wind farm is maximized. After 200 seconds, the change in the wind direction happens causing the downstream turbines to be partially in the wake of the upstream turbines. For case 2, $J^* = 5.1937 \times 10^7$ Watts and $u^* = [0.3333, \cdots, 0.3172]^\top$. That is $\forall i \in V_{G_d} : u_i^* = 0.3333$ while $\forall i \in V_{G_u} : u_i^* = 0.3172$. Again, from Figure 5, notice that the change in wind direction causes the downstream turbines to be fully in the wake of the upstream turbines. In both situations, the distributed TVESC is still able track and maximize the wind farm power capture.

5.3 Example 3

Again, consider the wind farm above. After 200 seconds, V_∞ decreases to 9.5 m/s and the wind direction changes 15°clockwise from the reference direction. With the same L, initial conditions and tuning parameters (except for σ that changes to 1×10^{-6} after 200 seconds), the technique is utilized to optimize the power generated. The simulation result for this example is presented in Figure 6.

5.4 Results

For example 3, $J^* = 4.4529 \times 10^7$ Watts and $u^* = [0.3333, \cdots, 0.3172]^\top$. That is $\forall i \in V_{G_d} : u_i^* = 0.3333$ while $\forall i \in V_{G_u} : u_i^* = 0.3172$. From Figure 6, it is seen that as V_∞ decreases, the wind farm power decreases. Additionally, the change in the wind direction (which introduces wake interactions) causes a further decrease in the power generation. Even with these changes, the distributed controllers are still able to track the optimum. This confirms the effectiveness of the technique.

6. CONCLUSION

In this paper, we have utilized a time-varying extremum seeking control technique for discrete-time systems in a distributed and a collaborative fashion to solve a wind farm power maximization problem. Additionally, this problem has been addressed over fixed and varying free stream wind speed and direction. Our results show the effectiveness and the technique. Although the main focus of this paper is on the control of wind farms, this technique can also be applied to other complex systems such as chemical, food, water treatment and pharmaceutical plants. Our next step is to address this problem over time -varying communication networks.

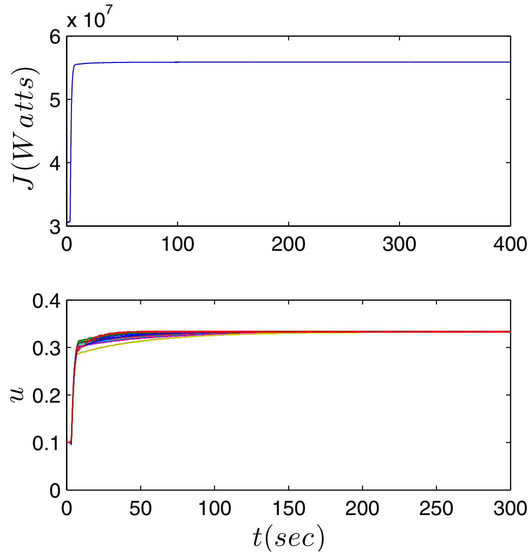

Fig. 3. Wind farm power and the axial induction factors over time at constant free stream wind speed and direction.

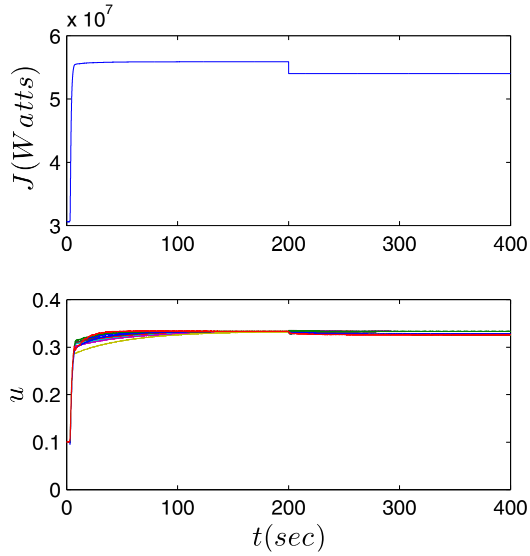

Fig. 4. Wind farm power and the axial induction factors over time at constant free stream wind speed and varying wind direction causing partial wake interactions.

REFERENCES

Chowdhury, S., Zhang, J., Messac, A., and Castillo, L. (2012). Unrestricted wind farm layout optimization: Investigating key factors influencing the maximum power generation. *Renewable Energy*, 38(1), 16–30. doi: 10.1016/j.renene.2011.06.033.

Chowdhury, S., Zhang, J., Messac, A., and Castillo, L. (2013). Optimizing the arrangement and the selection of turbines for wind farms subject to varying wind conditions. *Renewable Energy*, 52, 273–282. doi: 10.1016/j.renene.2012.10.017.

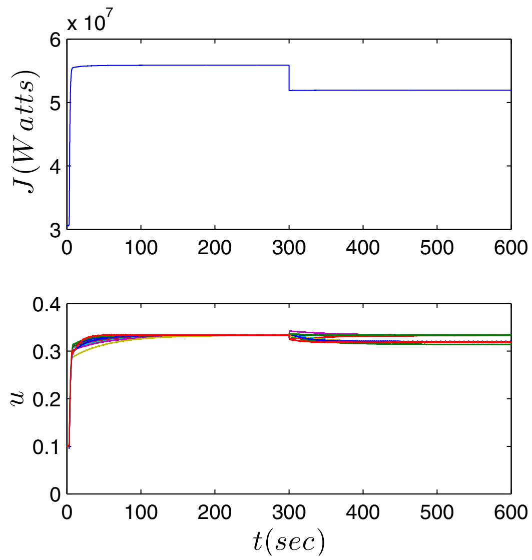

Fig. 5. Wind farm power and the axial induction factors over time at constant free stream wind speed and varying wind direction causing full wake interactions.

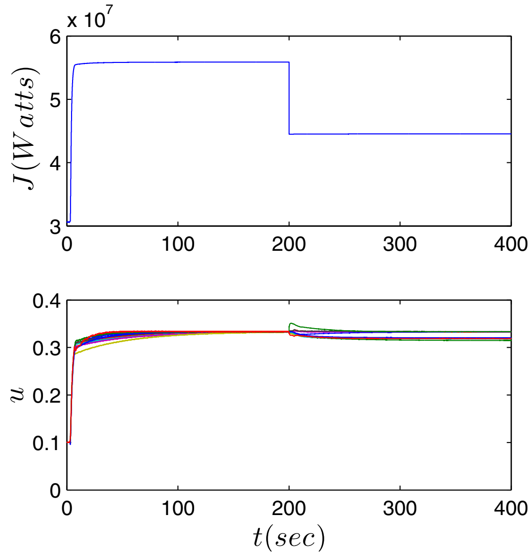

Fig. 6. Wind farm power and the axial induction factors over time at varying free stream wind speed and direction causing full wake interaction.

Dupont, B., Cagan, J., and Moriarty, P. (2016). An advanced modelling system for optimization of wind farm layout and wind turbine sizing using a multi-level extended pattern search algorithm. *Energy*, 106, 802–814. doi:10.1016/j.energy.2015.12.033.

Dupont, B.L. and Cagan, J. (2012). An extended pattern search approach to wind farm layout optimization. *Journal of Mechanical Design*, 134(8), 1–18. doi: 10.1115/1.4006997.

Freeman, R.A., Yang, P., and Lynch, K.M. (2006). Stability and convergence properties of dynamic average consensus estimators. In *Proceedings of the 45th IEEE Conference on Decision and Control*, 398–403. doi: 10.1109/CDC.2006.377078.

Ghods, N., Frihauf, P., and Krstić, M. (2010). Multi-agent deployment in the plane using stochastic extremum seeking. In *Proceedings of the 49th IEEE Conference on Decision and Control*, 5505–5510. doi: 10.1109/CDC.2010.5717282.

Goodwin, G.C. and Sin, K.S. (2013). *Adaptive Filtering Prediction and Control*. Dover Publications, New york.

Grunnet, J.D., Soltani, M., Knudsen, T., Kragelund, M.N., and Bak, T. (2010). Aeolus toolbox for dynamics wind farm model, simulation and control. In *Proceedings of European Wind Energy Conference and Exhibition, EWEC*.

Guay, M. (2014). A time-varying extremum-seeking control approach for discrete time systems. *Journal of Process Control*, 24(3), 98–112. doi: 10.1016/j.jprocont.2013.11.014.

Jensen, N.O. (1983). *A note on wind generator interaction*.

Liu, F. and Wang, Z. (2014). Offshore wind farm layout optimization using adapted genetic algorithm: A different perspective. *arXiv:1403.7178 [cs.NE]*.

Manwell, J.F., McGowan, J.G., and Rogers, A. (2002). *Wind Energy Explained: Theory, Design and Application*. Wiley, New york.

Marden, J.R., Ruben, S.D., and Pao, L.Y. (2013). A model-free appraoch to wind farm control using game theoretic methods. *IEEE Transactions on Control Systems Technology*, 21(4), 1207–1214. doi: 10.1109/TCST.2013.2257780.

Menon, A. and Baras, J.S. (2014). Collaborative extremum seeking for welfare optimization. In *Proceedings of the 53rd IEEE Conference on Decision and Control*, 346–351. doi:10.1109/CDC.2014.7039405.

Pérez, B., Mínguez, R., and Guanche, R. (2013). Offshore wind farm layout optimization using mathematical programming techniques. *Renewable Energy*, 53, 389–399. doi:10.1016/j.renene.2012.12.007.

Poveda, J. and Quijano, N. (2013). Distributed extremum seeking for real-time resource allocation. In *Proceedings of the 2013 American Control Conference*, 2772–2777. doi:10.1109/ACC.2013.6580254.

Sane, H.S., Haugstetter, C., and Bortoff, S.A. (2006). Building hvac control systems - role of controls and optimization. In *Proceedings of the 2006 American Control Conference*, 1121–1126. doi: 10.1109/ACC.2006.1656367.

Torres, P., van Wingerden, J., and Verhaegen, M. (2011). Modeling of the flow in wind farms for total power optimization. In *Proceedings of the 2011 IEEE International Conference on Control and Automation (ICCA)*, 963–968. doi:10.1109/ICCA.2011.6137984.

Troldborg, N., Sorensen, J.N., and Mikkelsen, R.F. (2010). Numerical simulations of wake characteristics of a wind turbine in uniform inflow. *Wind Energy*, 13(1), 86–99. doi:10.1002/we.345.

Vandermeulen, I., Guay, M., and McLellan, P.J. (2017). Formation control of high-altitude balloons experiencing real wind currents by discrete-time distributed extremum seeking control. In *Proceedings of the 2017 American Control Conference*, 991–996. doi: 10.23919/ACC.2017.7963082.

Zhang, C. and Ordóñez, R. (2012). *Extremum-seeking control and applications: A numerical optimization-based approach*. Springer London Dordrecht Heidelberg New York.